Thermodynamics of weakly coupled Falicov-Kimball chains from renormalization-group theory

Jozef Sznajd
Institute for Low Temperature and Structure Research, Polish Academy of Sciences, Wroclaw, Poland
(Received 1 October 2014; published 8 June 2015)

The linear perturbation renormalization group is used to study spinless two-band fermion chains at half-filling. The model consists of two species of spinless fermions, namely localized f and extended p, and it takes into account the following: the kinetic energy of fermions p, the on-site Coulomb repulsion V between p and f fermions, chemical potentials μ_p and μ_f adjusted in such a way that the average of the site occupation $\langle n_f^i\rangle + \langle n_p^i\rangle = 1$, and a weak interchain hopping t_x. The average occupation number, the specific heat, and the correlation functions are studied as functions of temperature. For a single chain the occupation number is a smooth function of T and the specific heat displays two maxima. The weak interchain hopping triggers a discontinuity in the occupation number of fermions as a function of temperature. A long-standing controversy on whether the Falicov-Kimball model can describe a discontinuous transition of n_f is also addressed.

DOI: 10.1103/PhysRevE.91.062111 PACS number(s): 05.30.Fk, 05.10.Cc

I. THE MODEL

Spinless fermions [1] can be considered as fully polarized electrons in a high magnetic field, but usually they are studied as a simplified model for the spin-$\frac{1}{2}$ fermions. Such a model is, of course, magnetically uninteresting, but it can still have interesting features associated with the effect of a competition between Coulomb repulsion and kinetic energy as well as interband mixing or charge ordering. For the single-band spinless model at half-filling and zero temperature, it is expected that a growth of the Coulomb repulsion leads to a transition from a metallic to an insulating charge-ordered state. The evaluation of physical quantities at finite temperature possesses some difficulties even for one-dimensional integrable models. The thermodynamics of such a model has been discussed by the thermodynamic Bethe ansatz and by the quantum transfer-matrix approach [2]. In our previous paper [3], we have used the linear renormalization-group transformation to study the weakly coupled chains of the spinless model, and we found the metal-insulator phase-transition temperature as a function of the interchain hopping parameter.

A single-band spinless model is not sufficient to describe all the relevant physics of the highly correlated electron systems. Therefore, to describe strong electron-electron correlations, several extensions and generalizations of the single-band spinless model have been proposed. And so, the spinless periodic Anderson model with phonons [4] and the extended Hubbard model with spinless itinerant and localized electrons [5–7] were used in the past for the description of the mixed-valance systems. The latter model in the limit of infinite dimensions was studied in the context of the metal-insulator transition [8]. The renormalization-group equation was derived for the two-band spinless fermion model in one dimension by Muttalib and Emery [9]. In this paper, we study the thermodynamic properties of the simplified two-band Hubbard model without hybridization, proposed by Falicov and Kimball [10] to describe the metal-semiconductor transitions in metallic oxides. The Falicov-Kimball model (FKM) is one of the simplest nontrivial interacting electron models, and since its creation it has attracted much attention in the literature. It has been used to study several phenomena, most commonly metal-insulator transitions [11,12], phase separation in the binary alloy [13], intermediate valence [14], and charge-density-wave order [15].

Except for very few rigorously controlled results in the strong-coupling regime and low temperature [16], much of the finite-temperature results for the FKM have either been based on the molecular field approximation, or they are restricted to one [17,18] or an infinite number of spatial dimensions [19]. Recently, the Suzuki-Takano renormalization-group transformation [20] combined with the Migdal-Kadanoff bond moving approximation [21] was used to find the phase diagram of the FKM [22]. The authors obtained the global phase diagram of the $d = 3$ FKM for a whole range of interactions (hopping, on-site Coulomb repulsion, and chemical potentials). However, they have not studied the temperature dependence of the thermodynamic quantities, and we should notice that the Migdal-Kadanoff approximation badly reproduces the physical content of the simplest $s = \frac{1}{2}$ field-free Heisenberg model, and it gives rather poor quantitative results even for the two-dimensional (2D) Ising model.

The model considered in this paper is composed of an infinite number of spinless fermion chains coupled by weak interchain hopping. The model consists of two species of spinless fermions, namely localized, denoted by f, and extended, p, and it can be defined by the following Hamiltonian:

$$H = H_0 + H_I, \tag{1}$$

where H_0 denotes a one-chain Hamiltonian,

$$H_0 = \tilde{t_p} \sum_{\langle ij\rangle} (p_i^\dagger p_j + p_j^\dagger p_i) + \tilde{V} \sum_i n_f^i n_p^i + \tilde{\mu_p} \sum_i n_p^i + \tilde{\mu_f} \sum_i n_f^i, \tag{2}$$

and

$$\tilde{t_p} = \frac{t_p}{T}, \quad \tilde{V} = \frac{V}{T}, \quad \tilde{\mu_i} = \frac{\mu_i}{T}, \tag{3}$$

$p_i^\dagger, p_i$ ($n_p^i = p_i^\dagger p_i$) are the creation and annihilation operators of the itinerant spinless fermions, and $f_i^\dagger, f_i$ ($n_f^i = f_i^\dagger f_i$) are the creation and annihilation operators for the spinless fermions in the localized state. A factor $-\beta = -1/k_B T$ has been absorbed in the Hamiltonian (1). Thus, $V < 0$ denotes

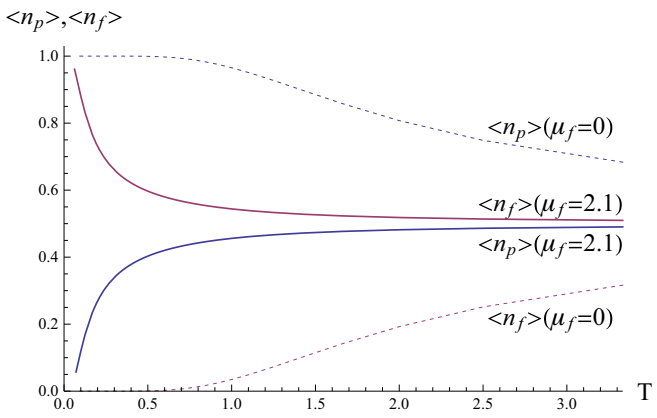

FIG. 1. (Color online) Averages of the site occupations $\langle n_i^f \rangle$ and $\langle n_i^p \rangle$ as functions of temperature for $t_p = 0$, $V = -4$ and $\mu_f = 0$ (dashed lines) and $\mu_f = 2.1$ (solid lines).

the repulsive Coulomb interaction. The first term in (2) is the kinetic energy corresponding to the hopping of the itinerant fermions p between sites i and j. The second term represents the on-site Coulomb repulsion between p itinerant and f localized fermions. μ_p and μ_f are chemical potentials adjusted in such a way that the average of the site occupation

$$\langle n_f^i \rangle + \langle n_p^i \rangle = 1. \tag{4}$$

In this paper, we assume that the localized level μ_f is temperature-independent and the condition (3) is fulfilled by calculating the chemical potential μ_p. For $t_p = 0$, the model (1) describes two classical subsystems (Ising models), both chemical potentials are temperature-independent, and the condition $\langle n_f^i \rangle + \langle n_p^i \rangle = 1$ is fulfilled for

$$\mu_f + \mu_p = -V. \tag{5}$$

In the symmetric case, $\mu_f = \mu_p = -V/2$, the average occupation numbers (AONs) $\langle n_f \rangle = \langle n_p \rangle = 1/2$, whereas for $\mu_f \neq \mu_p$ the AONs are temperature-dependent. In Fig. 1, the average occupation numbers for $t_p = 0$ and two cases: (i) $\mu_f = 0$, $\mu_p = -V$ and (ii) $\mu_f = 2.1$, $\mu_p = 1.9$, $V = -4$, are presented.

The interchain coupling is restricted to the hopping of the p fermions between the nearest-neighbor chains, and H_I reads

$$H_I = \tilde{t_x} \sum_{i,n} (p_{i,n}^\dagger p_{i,n+1} + p_{i,n+1}^\dagger p_{i,n}), \tag{6}$$

where n numbers the chains. In the following, all values will be given in units of t_p ($t_p = 1$).

The purpose of this paper is to use the linear perturbation renormalization group to study the thermodynamics: the specific heat, correlation functions, and average occupation number of the p fermions, as functions of temperature of the two-band spinless fermion model (FKM). The discontinuous transition of the p (f) -fermion occupation number $\langle n_p \rangle$ ($\langle n_f \rangle$) as a function of temperature is also discussed.

II. LINEAR PERTURBATION RENORMALIZATION GROUP

The linear perturbation renormalization-group (LPRG) approach starts with an approximate decimation of one chain (2). Then, on the basis of it the interchain interaction is renormalized in a perturbative way [23].

The RG transformation for the Hamiltonian (1) is defined by

$$e^{H'(\hat{\sigma},\hat{\phi})} = \mathrm{Tr}_p P(\hat{\sigma},\hat{\phi};\hat{p},\hat{f}) e^{H(\hat{p},\hat{f})} \tag{7}$$

with a linear weight operator $P(\hat{\sigma},\hat{\phi};\hat{p},\hat{f})$, which projects the original fermions p and f space onto the space of the new fermions σ and ϕ,

$$P(\hat{\sigma},\hat{\phi};\hat{p},\hat{f}) = \prod_{i=0} \left(1 + p_{mi+1}^\dagger \sigma_{i+1} + \sigma_{i+1}^\dagger p_{mi+1} + 2n_p^{mi+1} n_\sigma^{i+1} - n_p^{mi+1} - n_\sigma^{i+1}\right)$$
$$\times \left(1 + f_{mi+1}^\dagger \phi_{i+1} + \phi_{i+1}^\dagger f_{mi+1} + 2n_f^{mi+1} n_\phi^{i+1} - n_f^{mi+1} - n_\phi^{i+1}\right), \tag{8}$$

where $\sigma_i^\dagger, \sigma_i$ ($n_\sigma^i = \sigma_i^\dagger \sigma_i$) and $\phi_i^\dagger, \phi_i$ ($n_\phi^i = \phi_i^\dagger \phi_i$) are the creation and annihilation operators of the new spinless fermions. For a single chain (2), the transformation (7) and (8) is a Suzuki-Takano [20] -type decimation transformation. For instance, for $m = 2$ in each renormalization step, every other site survives, whereas for $m = 3$ every third site survives, and so on. To obtain effective interactions between the operators on surviving sites, for $m = 2$ a three-site block has to be considered, and generally an $(m + 1)$-site block for any m.

For an infinite number of chains, the RG transformation (7) can be written as

$$H' = \ln \mathrm{Tr}_{p,f} P e^{H_0 + H_I}. \tag{9}$$

For simplicity, from now on we omit arguments of the operators H and P. Due to the noncommutativity of several parts of the Hamiltonian, there is a necessity for an approximate decomposition of the exponential operator. The simplest second-order decomposition is given by the symmetric product [24]

$$e^{H_0 + H_I} \approx e^{\frac{H_0}{2}} e^{H_I} e^{\frac{H_0}{2}}. \tag{10}$$

The interchain interaction $\mathcal{H}_I$ is renormalized in a perturbative way, and if we confine ourselves to the second order in the cumulant expansion the transformation (9) can be rewritten as

$$H' = \ln z_0 + \tfrac{1}{2}(\langle H_I \rangle_P + \langle H_I \rangle_L)$$
$$+ \tfrac{1}{8}\left(\langle H_I^2 \rangle_P + 2\langle H_I^2 \rangle_{P-L} + \langle H_I^2 \rangle_L\right)$$
$$- \tfrac{1}{8}\left(\langle H_I \rangle_P^2 + 2\langle H_I \rangle_P \langle H_I \rangle_L + \langle H_I \rangle_L^2\right), \tag{11}$$

where

$$z_0 = \mathrm{Tr}_{p,f} P e^{H_0}, \quad \langle A\rangle_L = \frac{1}{z_0}\mathrm{Tr}_{p,f} P A e^{H_0},$$
$$\langle A\rangle_P = \frac{1}{z_0}\mathrm{Tr}_{p,f} P e^{H_0 A}, \quad \langle A^2\rangle_{P-L} = \frac{1}{z_0}\mathrm{Tr}_{p,f} P A e^{H_0} A. \tag{12}$$

In contrast to the one-band model [3], in the case of the Hamiltonian (2) the RG transformation generates new interactions even for a single chain. So, except for the four original parameters (2)—t_p, V, μ_p, and μ_f—in the renormalization procedure, the following eight new couplings come into play:

$$u_p n_p^i n_p^j, \quad u_f n_f^i n_f^j, \quad v n_p^i n_f^j, \quad g_1 n_p^i n_p^j n_f^i, \quad g_2 n_f^i n_f^j n_p^i,$$
$$g_4 n_f^i n_f^j n_p^i n_p^j, \quad g_p p_i^\dagger p_j n_f^i, \quad g_n p_i^\dagger p_j n_f^i n_f^j. \tag{13}$$

If one considers the chains in higher dimensions, the LPRG transformation (9) generates additional interactions. The number of these new interactions already in the lowest nontrivial order cumulant expansion is infinite for an infinite system [23,25]. So, the LPRG transformation is obtained by using several approximations: the abbreviation of the cumulant expansion (11), the truncation of the new interchain interactions generated by the transformation, the approximate decomposition of the exponential operator (10), and the block approximation used for one-dimensional decimation [20]. All of these approximations are high-temperature approximations. Thus, the LPRG is a reliable approach at rather high temperatures.

III. TWO-BAND SPINLESS FERMION CHAIN

As mentioned above, applying the transformation (7) with the projector (8) for any m to the single-chain Hamiltonian (2), one obtains a renormalized Hamiltonian $\mathcal{H}'$ for new fermion operators $(\sigma^\dagger,\sigma,\phi^\dagger,\phi)$ and renormalized parameters t_p', μ_p', μ_f', and V' with eight additional terms (12) generated by the transformation. So, one has to complete the original Hamiltonian (2) by those couplings, and finally consider the renormalization-group flow in 12-dimensional coupling parameter space. For $m = 3$ (four site block), the renormalized couplings read

$$t_p' = \frac{1}{2}\lg\frac{\lambda_5}{\lambda_4}, \quad \mu_f' = 2\lg\frac{\lambda_2}{f_0}, \quad \mu_p' = \lg\frac{\lambda_4\lambda_5}{f_0^2},$$
$$V' = \lg\frac{f_0^2\lambda_6\lambda_8}{\lambda_2^2\lambda_4\lambda_5} - \frac{f_V - f_v}{W}\lg\frac{\lambda_6}{\lambda_8}, \tag{14}$$

where

$$W = \sqrt{4f_{g_p}^2 + 8f_{g_p}f_{t_p} + 4f_{t_p}^2 + (f_V - f_v)^2}, \tag{15}$$

and λ_i are eigenvalues of the operator H_0,

$$\lambda_2 = f_0 + f_{\mu_f}, \quad \lambda_{4,5} = f_0 + f_{\mu_p} \mp f_{t_p},$$
$$\lambda_{6,8} = \tfrac{1}{2}\big(2f_0 + 2f_{\mu_p} + 2f_{\mu_f} + f_V + f_v \mp W\big), \tag{16}$$

with

$$f_0 = \mathrm{Tr}_{p,f} R_f R_p e^{H_0}, \quad f_t = \mathrm{Tr}_{p,f} p_1 p_4^\dagger e^{H_0},$$
$$f_{\mu_p} = \mathrm{Tr}_{p,f}(2n_{1p} + n_{4p} - 2n_{1p}n_{4p} - 1)R_f e^{H_0},$$
$$f_{\mu_f} = \mathrm{Tr}_{p,f}(2n_{1f} + n_{4f} - 2n_{1f}n_{4f} - 1)R_p e^{H_0}, \tag{17}$$
$$f_V = \mathrm{Tr}_{p,f}(2n_{1p} - 1)(1 - n_{4p})(2n_{1f} - 1)(1 - n_{4f})e^{H_0},$$

and

$$R_f = (1 - n_{1f} - n_{4f} + n_{1f}n_{4f}),$$
$$R_p = (1 - n_{1p} - n_{4p} + n_{1p}n_{4p}). \tag{18}$$

The other H_0 eigenvalues and formulas for the effective couplings generated by the RG transformation (u_p', u_f', v', g_1', g_2', g_4', g_p', and g_n') are presented in the Appendix.

We are now able to evaluate numerically the renormalization transformation (7) [the appropriate recursion relations are given by Eqs. (14) and (A3)]. The RG transformation allows us to find the thermodynamic properties of the system. The free energy per site can be calculated by using the following formula:

$$f = \sum_{n=1}^{\infty}\frac{\ln f_0\big(t_p^{(n)},\mu_p^{(n)},\mu_f^{(n)},V^{(n)},\dots\big)}{3^n}, \tag{19}$$

where "n" numbers the RG steps. Knowing the temperature dependence of the free energy, one can find the temperature dependences of the internal energy and specific heat but also the average occupation numbers and correlation functions on site i-$G_{p,f}$ and adjacent sites i,j-$G_{p,p}$,$G_{f,f}$:

$$G_{p,f} \equiv \langle n_p^i n_f^i\rangle, \quad G_{p,p} \equiv \langle n_p^i n_p^{i+1}\rangle, \quad G_{f,f} \equiv \langle n_f^i n_f^{i+1}\rangle. \tag{20}$$

The first step in the LPRG procedure is the choice of the block size. It is obvious that a renormalization-group transformation should preserve all symmetries of the original problem. This determines, to some extent, the choice of the block size. For example, if one wants to admit the possibility of the existence of a phase transition to the two-sublattice

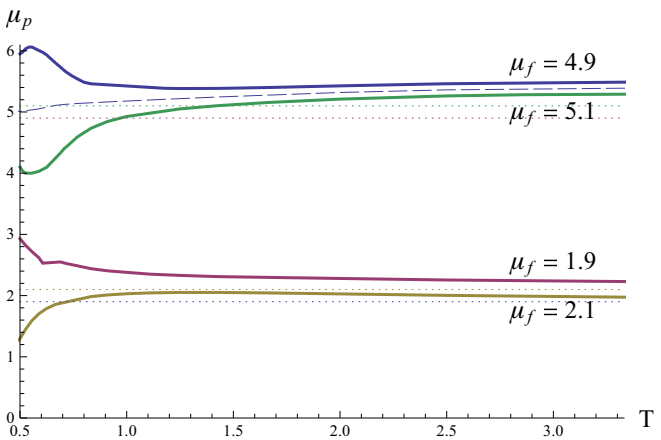

FIG. 2. (Color online) Temperature dependence of the chemical potential μ_p adjusted to fulfill the condition $\langle n_f\rangle + \langle n_p\rangle = 1$ for $t_p = 1$. Upper curves: $V = -10$, $\mu_f = 4.9$, 5.1, and 5 (dashed line) and bottom curves: $V = -4$ and $\mu_f = 1.9$ and 2.1.

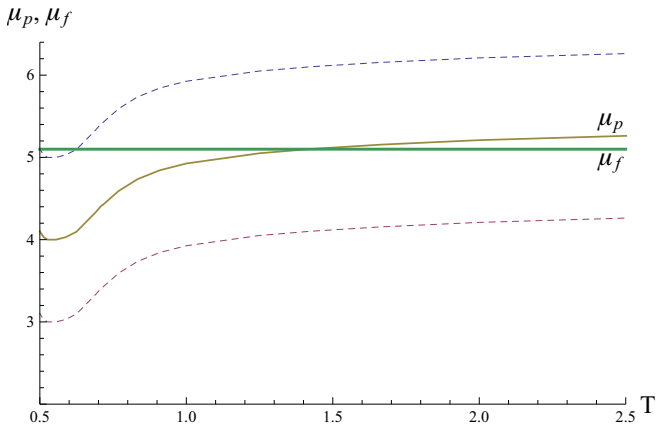

FIG. 3. (Color online) The chemical potentials μ_f and μ_p for the model with $V = -10$, $\mu_f = 5.1$, and the edges of the p-band (dashed lines).

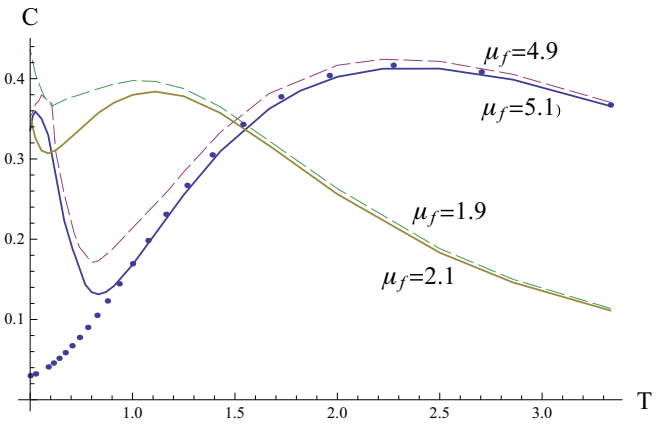

FIG. 5. (Color online) Temperature dependence of the one-chain specific heat for $t_p = 1$, (i) $V = -4$, $\mu_f = 1.9$, and 2.1 and (ii) $V = -10$, $\mu_f = 4.9$, 5.1, and 5 (dotted line).

phase, one should use blocks with an even number of sites (4,6,8, ...). The advantage from the use of a larger block was discussed in our previous article [3]. However, in this paper, taking into account a number of degrees of freedom for the two-band model, for simplicity, we will confine ourselves to the four-site block. As shown in Ref. [3], for such a block at very low temperature, some anomaly in thermodynamic functions is observed, which can be an artefact of neglecting quantum effects between adjacent blocks. So, due to the restricted validity of our procedure at low temperatures, all curves are only shown for the reduced temperature $T > 0.5$.

Using the recursion relations (14) and (A3), one can calculate the AON for a fixed value of μ_f and several values of μ_p and find for a given temperature the value of μ_p for which the relation $\langle n_f \rangle + \langle n_p \rangle = 1$ is fulfilled. In Fig. 2, the fitted chemical potential μ_p as a function of temperature is presented for two values of the Coulomb repulsion $V = -4$ with fixed values of $\mu_f = 1.9$ and 2.1 and $V = -10$ with $\mu_f = 4.9, 5.1$, and 5 (dashed line), all in units of t_p. The visible change in the temperature dependence of μ_p at lower temperature seems to be due to the proximity of μ_f to the p-band edge. For example, as seen in Fig. 3 for the model with $V = -10$ and $\mu_f = 5.1$, the p-band edge crosses the level f around $T = 0.63$. Evaluating numerically the recursion relation, one finds that the RG transformation exhibits only one high-temperature fixed point ($t_p^* = 0, V^* = \text{const}$) as one expects for a one-dimensional system, and the system does not undergo any finite-temperature phase transition. Now, using the formula (19) for the free energy per site, we can evaluate the average of the band occupation number, specific heat, and two-point correlation functions.

In Fig. 4, the average occupation numbers as functions of temperature are presented for two values of Coulomb repulsion: (i) $V = -4$ with $\mu_f = 1.9$ and 2.1; (ii) $V = -10$ with $\mu_f = 4.9, 5.1$, and 5. According to the convention adopted in this paper, where negative V corresponds to the repulsive Coulomb interactions, for $\mu_f > -\frac{1}{2}V$ the p fermions are transferred to the localized state f, and vice versa for $\mu_f < -\frac{1}{2}V$ the localized fermions are transferred to the band with decreasing temperature. As seen in the first case (i) $V = -4$ (left plot), this transfer is smooth, and for $\mu_f > -\frac{1}{2}V$ ($\mu_f < -\frac{1}{2}V$), $n_p > n_f$ ($n_p < n_f$) over the whole range of temperature (from now on we omit the brackets and denote an average as n_α, $\alpha = f$ or p). For larger coupling (ii) $V = -10$

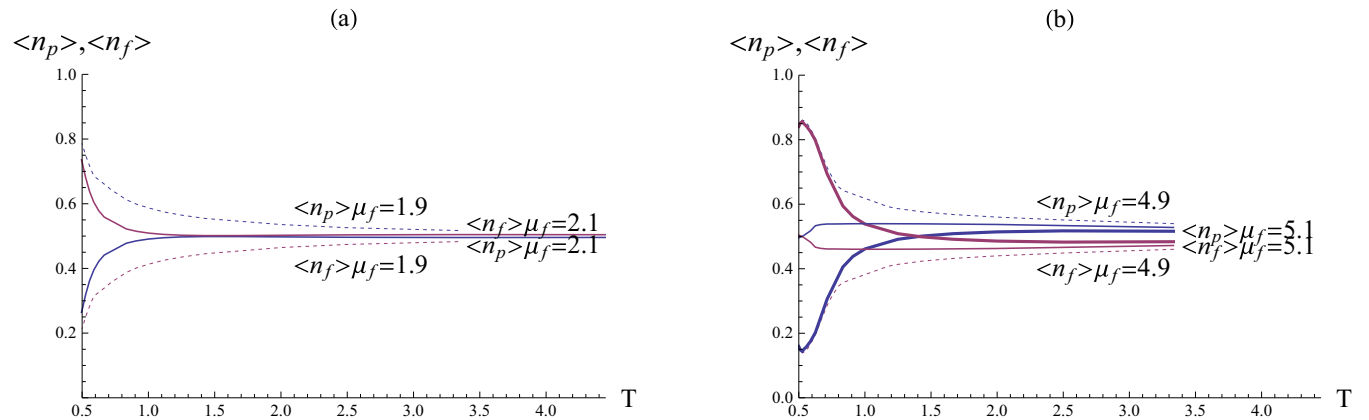

FIG. 4. (Color online) Averages of the site occupation as functions of temperature for $t_p = 1$, (a) $V = -4$ ($\mu_f = 1.9, 2.1$) and (b) $V = -10$ and $\mu_f = 4.9$, 5.1, and 5 (thin lines; the upper one denotes $\langle n_p \rangle$).

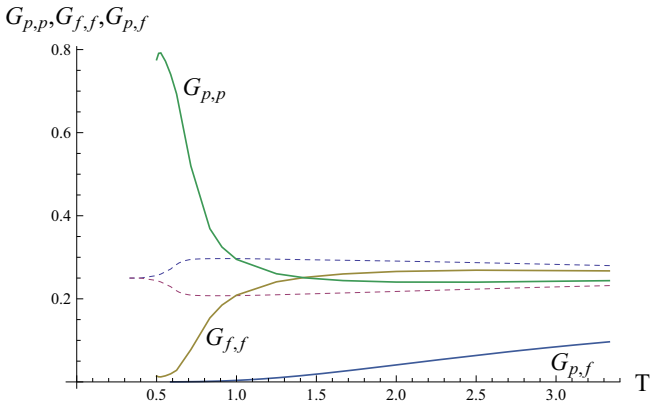

FIG. 6. (Color online) Temperature dependence of the correlation functions for $t_p = 1, V = -10$ and $\mu_f = 5.1$ (solid lines) and $\mu_f = 5$ (dotted lines, upper one denotes $G_{p,p}$).

(right plot), we consider three cases. For $\mu_f = -\frac{1}{2}V = 5$ the occupation numbers n_p and n_f are almost temperature-independent over a wide temperature range. However, due to the hopping term, $n_p > n_f$ for $T > T_{\rm eq} = 0.525$. At $T = T_{\rm eq}$, the curves $n_\alpha(T)$ intersect and then both AON tend to the value $n_p = n_f = \frac{1}{2}$. For $\mu_f = 4.9 < -\frac{1}{2}V$ similarly to the weaker coupling case ($V = -4$), $n_p > n_f$ over the whole range of temperature. In contrast, for $\mu_f = 5.1 > -\frac{1}{2}V$ at high temperature $n_p > n_f$, the occupation numbers are equal to each other at $T_{\rm eq} = 1.41$ and then $n_f > n_p$, as expected.

The specific heat as a function of temperature for the same models is presented in Fig. 5. For the symmetric case, $\mu_f = -\frac{1}{2}V = 5$, the specific-heat curve has a single broad maximum. In other cases, the specific heat displays two maxima and a minimum, the depth of which depends on the coupling strength. A two-maxima structure of the specific heat is also observed in the standard one-dimensional Hubbard model with $U > 4t$, and the minimum corresponds to a maximum in the electronic localization [3]. In the present model, the minima correspond to the maxima in the fermion transfer from the p-band to the f-level (for $\mu_f > -\frac{1}{2}V$) or vice versa from the f-level to the p-band (for $\mu_f < -\frac{1}{2}V$). As seen in Fig. 4, at high temperatures the average occupation numbers weakly depend on temperature (the transfer between bands is slow) down to a certain temperature at which the transfer rapidly increases. The same two-peak specific-heat structure with a sharp peak followed by a broad peak was found for one-dimensional FKM within small cluster exact-diagonalization calculations [17].

Next, we use the RG transformation to find the two-particle on-site $G_{p,f}$ and nearest-neighbor (NN) $G_{f,f}$ and $G_{p,p}$ correlation functions (20). In Fig. 6, their temperature dependences are shown for $V = -10$ and $\mu_f = 5$ and 5.1. At high temperatures, all functions tend to $\frac{1}{4}$, which means $\frac{1}{2}$ p-particle and $\frac{1}{2}$ f-particle per site, as expected. At low temperature, the on-site function $G_{p,f}$ monotonically goes to zero in both cases $\mu_f = 5$ and 5.1. Instead, the NN function $G_{p,p}$ for the symmetric case $\mu_f = 5$ first slightly increases from $\frac{1}{4}$($G_{f,f}$ decreases) and then tends again to $\frac{1}{4}$. For $\mu_f = 5.1$, $G_{p,p}$ tends to zero.

IV. COUPLED FERMION CHAINS

Below in this section, we shall use the LPRG to study a system with an infinite number of spinless fermion chains at finite temperature, where the chains are coupled by the weak interchain single-particle hopping t_x (6). As was mentioned above, the LPRG transformation when applied on an infinite system generates an infinite number of new interactions already in the lowest nontrivial order of the cumulant expansion. Thus, in order to find the renormalized Hamiltonian, we have to confine ourselves to a finite cluster. In a second-order calculation, one has to consider three rows. We use a cluster with four sites in each row ($4-4-4$). So the sites from the first and third rows (odd rows) are decimated such that in each RG step every third site survives, whereas sites from the second row (even row) are removed (the trace is taken over all sites) [23]. In addition, for simplification we will consider only two-site interchain interactions, thereby neglecting four-site interactions which appear for the ($4-4-4$) cluster. Under such an assumption, the LPRG transformation generates only one new interaction—an interchain diagonal hopping,

$$t_y \sum_{i,n} (p^\dagger_{i,n} p_{i+1,n+1} + p^\dagger_{i+1,n+1} p_{i,n}). \tag{21}$$

Hence, in the second-order cumulant expansion for the cluster ($4-4-4$), one has to evaluate the averages (11) of H_I^2,

$$\langle H_I^2 \rangle_\alpha = \left\langle \left(\sum_{n=0}^{2} \sum_{i=1}^{4} [t_x (p^\dagger_{i,n} p_{i,n+1} + p^\dagger_{i,n+1} p_i) + t_y (p^\dagger_{i,n} p_{i+1,n+1} + p^\dagger_{i+1,n+1} p_{i,n})] \right)^2 \right\rangle_\alpha , \tag{22}$$

which means the averages of several fermion operators products, e.g.,

$$t_x^2 \left\langle \sum_{i=1}^{4} p_i^\dagger P_i P_{i+1}^\dagger p_{i+1} \right\rangle, \tag{23}$$

where in Eq. (22) the operators $p^\dagger, p$ refer to the decimated (odd) rows, and operators denoted by upper-case $P^\dagger, P$ refer to the removed (even) rows. These averages have rather complicated expressions, and as an example we present the appropriate formula for (23) in the Appendix.

Now, the transformation (11) allows us to find 14 renormalized parameters: four single-chain couplings t_p', μ_p', μ_f', V' (2), eight created by RG for the single chain (13), and two interchain t_x', t_y' as functions of the original parameters. Knowing the recursion relations for the interaction parameters, one can evaluate numerically the LPRG transformation for the Hamiltonian (1) defined by the original parameters t_p, V, μ_p, μ_f, and t_x and analyze a flow in 14-dimensional

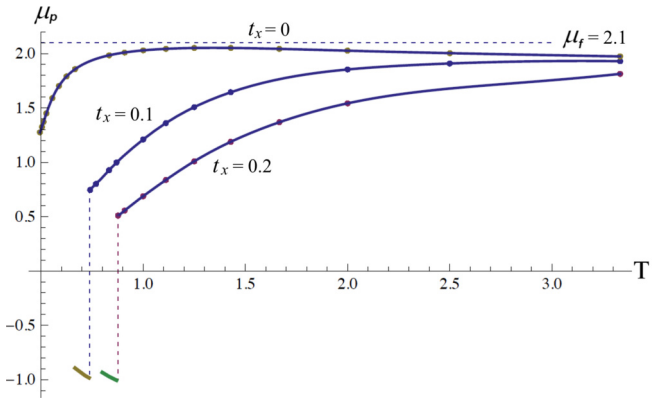

FIG. 7. (Color online) Temperature dependence of the weakly coupled chain chemical potential μ_p for $t_p = 1$, $V = -4$, and $t_x = 0$, 0.1, and 0.2 (from top to bottom).

coupling parameter space. Now again, we have to find the chemical potential μ_p for which the condition $\langle n_p\rangle + \langle n_f\rangle = 1$ is fulfilled (μ_f is assumed to be constant). The results are presented in Fig. 7 for two values of the interchain coupling $t_x = 0.1$ and 0.2 and compared with the chemical potential of a single chain. Next we are able to evaluate the specific heat.

At this stage, it is worthwhile to remind ourselves of the LPRG results for the two-dimensional one-band spinless fermion model at half-filling ($\mu_p = -u_p$) [3] given by the Hamiltonian

$$H = t_p \sum_{\langle ij\rangle} (p_i^\dagger p_j + p_j^\dagger p_i) + u_p \sum_i n_p^i n_p^{i+1} + \mu_p \sum_i n_p^i + t_x \sum_{i,n} (p_{i,n}^\dagger p_{i,n+1} + p_{i,n+1}^\dagger p_{i,n}), \quad (24)$$

where n numbers chains.

For $t_x \neq 0$ and $T > T^*$, the RG flow is toward a $T = \infty$ fixed point $t_p^* = 0, t_x^* = 0$ (solid lines in Fig. 8), which describes a disordered phase, whereas for $T < T^*$ (dashed lines) the coupling parameter t_x diverges ($t_x \to -\infty$). The temperature $T^* = T_c$ can be interpreted as a critical temperature between a disordered phase where the average occupation number of the p fermions is the same for all sites, and a

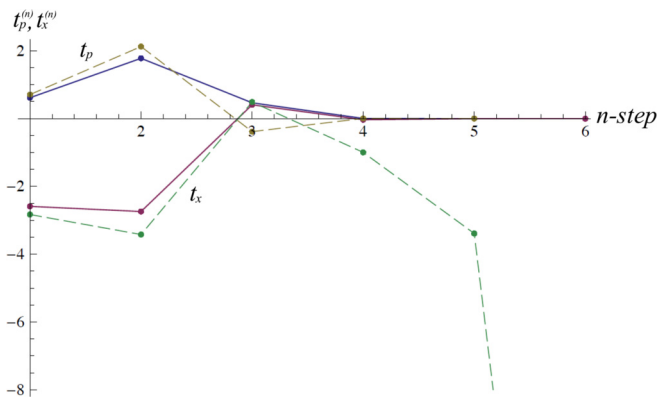

FIG. 8. (Color online) The iteration of the parameters t_p and t_x at $T > T^*$ (solid lines) and $T < T^*$ (dashed lines) for the single-band model (24).

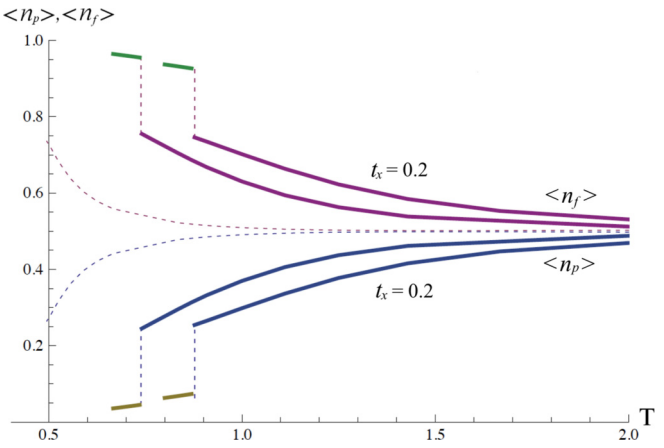

FIG. 9. (Color online) Temperature dependences of the coupled chain occupation numbers $\langle n_f\rangle$ and $\langle n_p\rangle$ for $t_p = 1$, $V = -4$, $\mu_f = 2.1$, and $t_x = 0$ (dashed line) and $t_x = 0.1$ and 0.2 (solid lines).

charge-ordered phase where this number is different in every other site in a chain. The critical temperature corresponds to the specific-heat divergence as seen in Fig. 10 (dashed lines). Notice that in the model (24) as well as in the present model, there is no Coulomb interaction between the chains, which are coupled only by the hopping t_x. Thus, the weak interchain hopping in the one-band case triggers a charge-ordering continuous phase transition.

Let us now turn to the two-band model described by the Hamiltonian (1). As presented in Fig. 7, contrary to the one-dimensional case for the coupled chains μ_p for which the condition (3) is fulfilled, there is a smooth function of T only if the temperature is higher than some $T_b = T(t_x)$ ($T_b \approx 0.74$ for $t_x = 0.1$ and $T_b \approx 0.88$ for $t_x = 0.2$). Technically, if we start with some values of the original parameters, for example $\mu_p = 2.1$, $V = -4$, $t_p = 1$, $t_x = 0.1$, and iterate the recursion relations for several values of μ_p at a given temperature, we can find a value of μ_p that leads to $\langle n_p\rangle + \langle n_f\rangle = 1$. It appears that such a continuous solution exists only for $T \geqslant T_b$. At $T = T_b$,

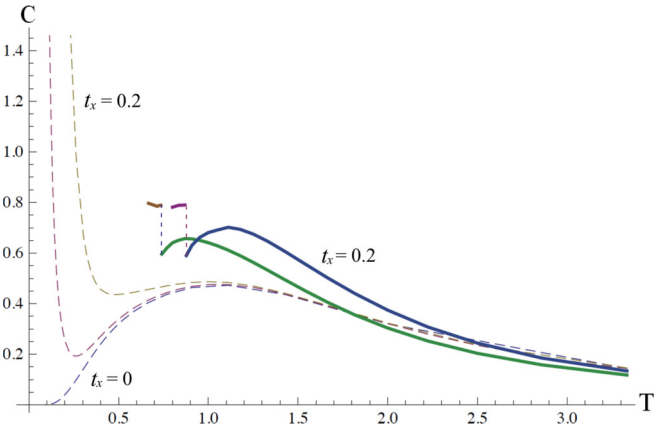

FIG. 10. (Color online) Temperature dependence of the coupled chain specific heat for $t_p = 1$, $V = -4$, $\mu_f = 2.1$, and $t_x = 0.1$ and 0.2 (solid lines). For comparison, the specific heat for a single-band system at half-filling with $t_p = 1$, $u_p = -4$, and $\mu_p = 4$ for $t_x = 0$, 0.1, and 0.2 is presented (dashed lines).

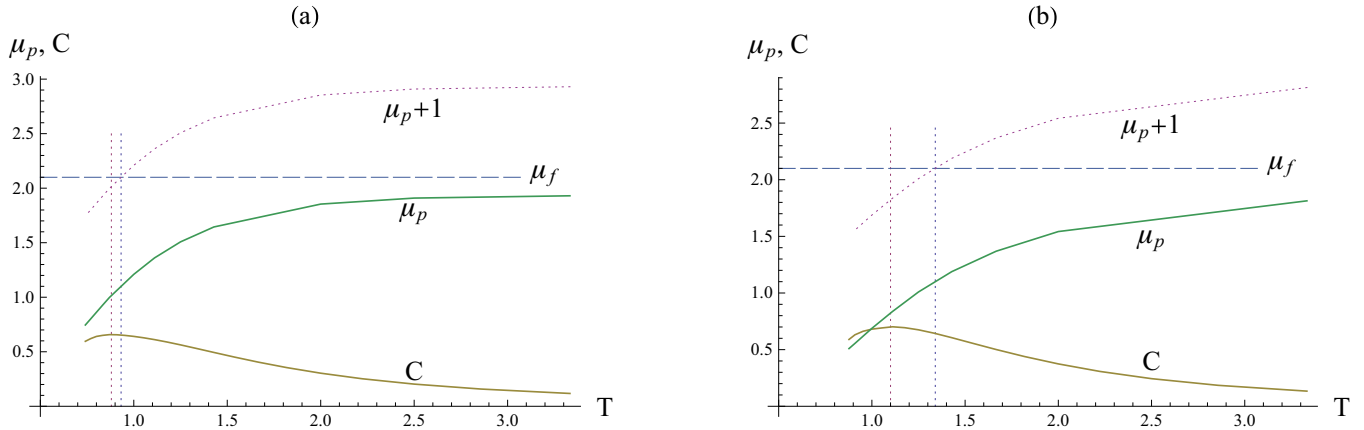

FIG. 11. (Color online) Temperature dependence of the coupled chain chemical potentials and specific heat for $t_p = 1$, $V = -4$, $\mu_f = 2.1$, and $t_x = 0.1$ (a) and $t_x = 0.2$ (b).

the solution for μ_p undergoes a jump and consequently the discontinuity in occupation number is observed (Fig. 9). This supports the claim that the FK model can describe the discontinuous transitions of the p- (f-) fermion occupation number as a function of temperature [26] at least for the weakly coupled chains. The value of the jump decreases upon increasing the interchain coupling t_x. Unfortunately, within the present approximation we are not able to decide if the jump vanishes for the isotropic case ($t_x = t_p$).

In Fig. 10, the specific-heat curves of the present model are compared with the results for the weakly coupling chains of the one-band spinless fermion model [3]. As seen in the latter case, the specific heat diverges for a finite value of the coupling parameter t_x as expected at the critical point. For small interchain coupling ($t_x = 0.1$), this divergence is preceded by the hump as a trace of the quasi-one-dimensional character of the system. The hump disappears for larger t_x, and for $t_x = 0.2$ it is almost invisible. On the contrary, in the present model there is no indication of the continuous phase transition at finite temperature. The specific heat shows a maximum below the temperature at which the band edge ($\mu_p - 1$) crosses the level μ_f (Fig. 11) and the discontinuity at $T = T_b$ due to the jump of the occupation number.

V. SUMMARY

First, the one-dimensional two-band spinless fermion model with p-fermion hopping term t_p, on-site Coulomb repulsion V, and chemical potentials μ_p,μ_f with one electron per site (Falicov-Kimball model) has been studied by means of the linear renormalization-group transformation. The chemical potential μ_p has been determined self-consistently by taking into account the conservation of the total number of electrons. The method should lead to reasonable results for t_p not too large (compared with V) and at high temperature. Therefore, two cases have been considered: (i) $|V| = 4t_p$ and (ii) $|V| = 10t_p$ at reduced temperature $T > 0.5$. In both cases, the value of μ_f has been fixed to be slightly below and above $-V/2$. In the first case (i) $\mu_f = 1.9$ and 2.1 ($V = -4$,$t_p = 1$) and in the second case (ii) $\mu_f = 4.9$ and 5.1 ($V = -10$). At high temperature, the chemical potential is almost temperature-independent, especially for the weaker coupling ($V = -4$) over a wide temperature interval. At lower temperature, the character of the temperature dependence of μ_p clearly changes (Fig. 2), and the transfer of electrons between the bands rapidly increases (Fig. 4). In all cases, the occupation numbers are smooth functions of T as expected; only in the case of strong coupling ($V = -10$) and $\mu_f = 5.1 > -\frac{1}{2}V$ do the occupation number curves $n_f(T)$ and $n_p(T)$ intersect at $T \approx 1.41$. The specific-heat curves exhibit a two-maximum structure found previously for the same model by the small-cluster exact-diagonalization calculations [17].

For higher dimension, the question of whether the discontinuous transition of the occupation number as a function of temperature occurs in FKM is still an issue of interest. This question was discussed in the review article of Freericks and Zlatić [19]. The charge-transfer transition in which the character of the electronic states is unchanged, but their occupancy is shifted from an itinerant to a localized band in FKM, was first studied by Falicov, Kimball, and Ramirez [11,26]. Within the molecular field approximation (MFA), they showed that the occupation number n_f for some values of the coupling parameter undergoes a jump at finite temperature. However, in the presumably better approximation (e.g., the coherent-potential approximation), for the same values of the parameters, n_f is a smooth function of T [12,27]. No discontinuous transition at finite temperature has been found by using small-cluster exact-diagonalization calculations [17]. Later, Chung and Freericks [28] showed that for an infinite-coordination Bethe lattice, a first-order charge-transfer phase transition can be observed for a narrow value range of the Coulomb interaction. The first-order phase transition has also been observed by using the Monte Carlo method in the weak interaction regime [29].

In this paper, to study FKM chains we employed the LPRG method on the $(4-4-4)$-cluster by confining ourselves to two-site interactions only. We have assumed that the chains are coupled by a weak single-particle hopping. Also in this case, the chemical potential μ_p is determined by the condition $n_p + n_f = 1$. However, for the weakly coupled chains, the LPRG recursion relations lead to the solution for μ_p, which has a jump. Consequently, there is a discontinuity in the occupation number as a function of temperature (Fig. 9). The value of the jump is smaller for higher interchain hopping, and within the

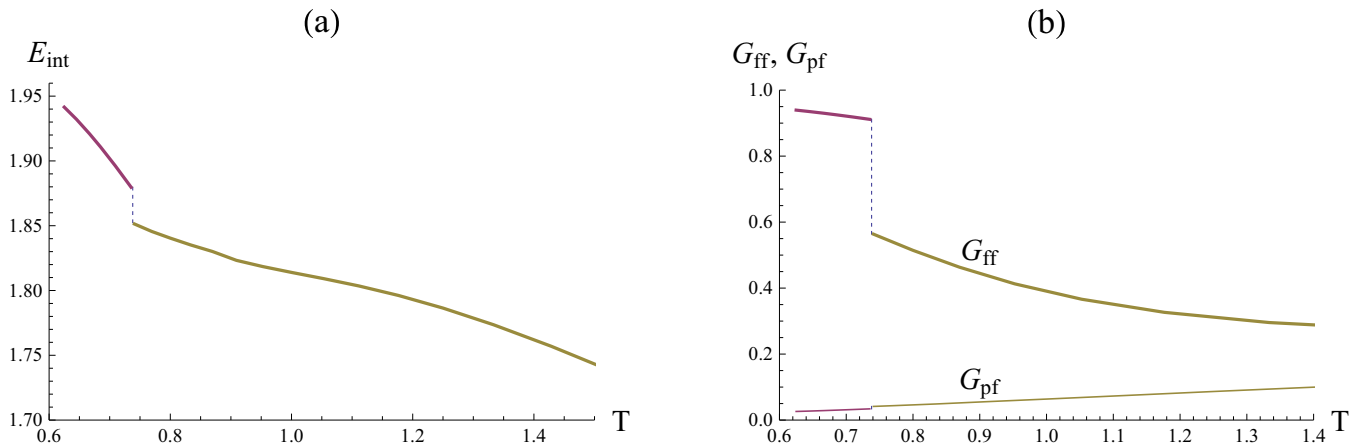

FIG. 12. (Color online) Temperature dependences of the coupled chain internal energy (a) and correlation functions G_{ff},G_{pf} (b) for $t_p = 1$, $V = -4$, $\mu_f = 2.1$, and $t_x = 0.1$.

present approximation we cannot decide whether a finite jump would also remain for the isotropic system with $t_x = t_p$. The present approach does not permit us to analyze a system below a critical point or spinodal, however we have found discontinuity in the occupation number (Fig. 9) and jumps of the internal energy (Fig. 12) and the on-site $G_{pf} = \langle n_p^i n_f^i \rangle$ and nearest-neighbor $G_{ff} = \langle n_f^i n_f^{i+1} \rangle$ correlation functions (Fig. 12). This indicates a discontinuous transition in which the electrons are transferred from the "p" band to the localized "f" level.

Thus, we conclude that the weakly coupled Falicov-Kimball chains with one electron per site ($n_f + n_p = 1$) undergo a finite-temperature charge-transfer discontinuous phase transition in which for $\mu_f > -\frac{1}{2}V$, fermions are shifted from an itinerant to a localized band.

APPENDIX

1. Recursion relations for a single chain

The eigenvalues of the single-chain Hamiltonian (2) completed by the couplings (12) generated by the RG transformation have the form

$$\begin{aligned}
&\lambda_{10} = f_0 + 2f_{\mu_f} + f_{u_f}, \quad \lambda_{(11,12)} = f_0 + f_{g_2} \mp f_{g_n} \mp 2f_{g_p} + 2f_{\mu_f} + f_{\mu_p} \mp f_{t_p} + f_V + f_v + f_{u_f},\\
&\lambda_{13} = f_0 + 2f_{\mu_p} + f_{u_p}, \quad \lambda_{14} = f_0 + 2f_{g_1} + f_{\mu_f} + 2f_{\mu_p} + f_V + f_v + f_{u_p},\\
&\lambda_{16} = f_0 + 2f_{g_1} + 2f_{g_2} + f_{g_4} + 2f_{\mu_f} + 2f_{\mu_p} + 2f_V + 2f_v + f_{u_f} + f_{u_p},
\end{aligned} \tag{A1}$$

where

$$\begin{aligned}
f_v &= \mathrm{Tr}_{p,f}(2n_{1p} - 1)(1 - n_{4p})(2n_{4f} - 1)(1 - n_{1f})e^{H_0},\\
f_{u_p} &= \mathrm{Tr}_{p,f}(2n_{1p} - 1)(2n_{4p} - 1)P_f e^{H_0},\\
f_{u_f} &= \mathrm{Tr}_{p,f}(2n_{1f} - 1)(2n_{4f} - 1)P_p e^{H_0},\\
f_{g_1} &= \mathrm{Tr}_{p,f}(2n_{1p} - 1)(2n_{4p} - 1)(1 - n_{1f})(2n_{4f} - 1)e^{H_0},\\
f_{g_2} &= \mathrm{Tr}_{p,f}(2n_{1p} - 1)(1 - n_{4p})(2n_{1f} - 1)(2n_{4f} - 1)e^{H_0},\\
f_{g_4} &= \mathrm{Tr}_{p,f}(2n_{1p} - 1)(2n_{4p} - 1)(2n_{1f} - 1)(2n_{4f} - 1)e^{H_0},\\
f_{g_p} &= \mathrm{Tr}_{p,f}\, p_1 p_4^\dagger (2n_{1f} - 1)(1 - n_{4f})e^{H_0},\\
f_{g_n} &= \mathrm{Tr}_{p,f}\, p_1 p_4^\dagger (2n_{1f} - 1)(2n_{4f} - 1)e^{H_0}.
\end{aligned} \tag{A2}$$

and renormalized couplings are

$$\begin{aligned}
v' &= \frac{1}{2}\lg\frac{f_0^2}{\lambda_2^2\lambda_4\lambda_5} + \frac{f_V - f_v}{2Q}\lg\frac{\lambda_6}{\lambda_8} + \frac{1}{2}\lg(\lambda_6\lambda_8), \quad u_p' = \lg\frac{f_0\lambda_{13}}{\lambda_4\lambda_5}, \quad u_f' = \lg\frac{f_0\lambda_{10}}{\lambda_{12}^2},\\
g_1' &= \lg\frac{\lambda_4\lambda_5\lambda_{12}\lambda_{14}}{f_0\lambda_{13}\lambda_{16}\lambda_{18}}, \quad g_2' = \frac{1}{2}\lg\frac{\lambda_2^4\lambda_4\lambda_5\lambda_8\lambda_{11}}{f_0^2\lambda_{10}^2\lambda_6^2\lambda_8^2} - R\lg(\lambda_{12}),
\end{aligned}$$

$$g_4' = \lg \frac{f_0\lambda_6^2\lambda_8^2\lambda_{10}\lambda_{12}\lambda_{13}\lambda_{16}}{\lambda_2^2\lambda_4\lambda_5\lambda_{11}\lambda_{14}^2} + R\lg(\lambda_{12}), \quad g_p' = \frac{1}{2}\lg\frac{\lambda_4}{\lambda_5} - \frac{f_{g_p}+f_{t_p}}{W}\lg\frac{\lambda_6}{\lambda_8},$$
$$g_n' = \frac{1}{2}\lg\frac{\lambda_5}{\lambda_4\lambda_{11}} + \frac{2(f_{g_p}+f_{t_p})}{W}\lg\frac{\lambda_6}{\lambda_8} - \frac{1}{2}R\lg(\lambda_{12}), \quad R = \frac{f_{g_n}+2f_{g_p}+f_{t_p}}{f_{g_n}-2f_{g_p}-f_{t_p}}. \tag{A3}$$

2. Coupled chains

To evaluate the transformation (10), one has to know the averages of the products of the original fermion operators from the decimated (p) and removed (P) rows of a type $\langle p_i^\dagger P_k P_l^\dagger p_j\rangle$. All of them are expressed through the effective fermion operators ($\sigma^\dagger,\sigma,\phi^\dagger,\phi$) and, for example,

$$\left\langle \sum_{i=1}^{4} p_i^\dagger P_i P_{i+1}^\dagger p_{i+1} \right\rangle = -\sum_{i=1}^{4}\langle p_i^\dagger p_{i+1}\rangle\langle P_{i+1}^\dagger P_i\rangle = -r_1\langle\hat{Q}\rangle$$
$$= -r_1\big(Q_{10} + Q_{\mu_p}\big(n_\sigma^{(1)}+n_\sigma^{(2)}\big) + Q_{\mu_f}\big(n_\phi^{(1)}+n_\phi^{(2)}\big) + Q_{u_p}\big(n_\sigma^{(1)}n_\sigma^{(2)}\big) + Q_{u_f}\big(n_\phi^{(1)}n_\phi^{(2)}\big)$$
$$+ Q_V\big(n_\sigma^{(1)}n_\phi^{(1)} + n_\sigma^{(2)}n_\phi^{(2)}\big) + Q_v\big(n_\sigma^{(1)}n_\phi^{(2)} + n_\sigma^{(2)}n_\phi^{(1)}\big) + Q_{t_p}(\sigma_1^\dagger\sigma_2 + \sigma_2^\dagger\sigma_1)\big), \tag{A4}$$

where

$$\hat{Q} = \sum_{i=1}^{4} p_i^\dagger p_{i+1}, \tag{A5}$$

and

$$Q_{10} = C_0 Z_0, \quad Q_{\mu_k} = C_{\mu_k}Z_0 + C_0 Z\mu_k + C_{\mu_k}Z_{\mu_k} \quad (k=p,f),$$
$$Q_{u_k} = C_0 Z_{u_k} + 2C_{\mu_k}\big(Z_{\mu_k}+Z_{u_k}\big) + C_{u_k}\big(Z_0+2Z_{\mu_k}+Z_{u_k}\big),$$
$$Q_V = C_{\mu_f}Z_{\mu_p} + \big(C_0+C_{\mu_f}\big)Z_V + C_{\mu_p}\big(Z_{\mu_f}+Z_V\big) + C_V\big(Z_0+Z_{\mu_f}+Z_{\mu_p}+Z_V\big),$$
$$Q_v = C_{\mu_p}Z_{\mu_f} + C_{\mu_f}Z_{\mu_p} + C_v\big(Z_0+Z_{\mu_p}+Z_{\mu_f}\big), \tag{A6}$$

with

$$Z_0 = \mathrm{Tr}_{p,f}\,\hat{Q}R_f R_p e^{H_0}, \quad Z_{\mu_k} = \mathrm{Tr}_{p,f}\,\hat{Q}(2n_{1k}-1)(1-n_{4k})R_k e^{H_0},$$
$$Z_{u_k} = \mathrm{Tr}_{p,f}\,\hat{Q}(2n_{1k}-1)(2n_{4k}-1)R_{k'}e^{H_0},$$
$$Z_{V,v} = \mathrm{Tr}_{p,f}\,\hat{Q}(1-2n_{1p})(1-n_{4p})(1-n_{(4,1)f})e^{H_0},$$
$$Z_{t_p} = \mathrm{Tr}_{p,f}\,\hat{Q}p_1 p_4^\dagger e^{H_0} \quad (k,k'=p,f),$$
$$C_0 = \frac{1}{f_0}, \quad C_{\mu_p} = \frac{1}{\lambda_4}+\frac{1}{\lambda_5}-\frac{2}{f_0}, \quad C_{\mu_f} = 2\left(\frac{1}{\lambda_2}-\frac{1}{f_0}\right), \quad C_{t_p} = \frac{1}{2}\left(\frac{1}{\lambda_5}-\frac{1}{\lambda_4}\right),$$
$$C_V = \frac{2}{f_0}-\frac{2}{\lambda_2}-\frac{1}{\lambda_4}-\frac{1}{\lambda_5}+\frac{1}{\lambda_6}+\frac{1}{\lambda_8}+\frac{f_v-f_V}{\lambda_6\lambda_8},$$
$$C_v = \frac{1}{f_0}-\frac{1}{\lambda_2}-\frac{\lambda_4+\lambda_5}{2\lambda_4\lambda_5}+\frac{f_v-f_V+\lambda_6+\lambda_8}{2\lambda_6\lambda_8}. \tag{A7}$$

For the decimated rows, the single chain averages are given by

$$\langle P_1^\dagger P_{1+\alpha}\rangle = \frac{\mathrm{Tr}[P_1^\dagger P_{1+\alpha}e^{H_0}]}{\mathrm{Tr}[e^{H_0}]}. \tag{A8}$$

[1] W. Kohn, Phys. Rev. Lett. **19**, 789 (1967).
[2] K. Sakai, M. Shiroishi, J. Suzuki, and Y. Umeno, Phys. Rev. B **60**, 5186 (1999).
[3] J. Sznajd and K. W. Becker, J. Phys.: Condens. Matter **17**, 7359 (2005).
[4] N. Grewe, P. Entel, and H. J. Leder, Z. Phys. B **30**, 393 (1978).
[5] P. Schlottmann, Phys. Rev. B **22**, 613 (1980).
[6] W. Hanke and J. E. Hirsch, Phys. Rev. B **25**, 6748 (1982).
[7] M. Barma, J. Phys. C **15**, 721 (1982).
[8] Q. Si, M. J. Rozenberg, G. Kotliar, and A. E. Ruckenstein, Phys. Rev. Lett. **72**, 2761 (1994).
[9] K. A. Muttalib and V. J. Emery, Phys. Rev. Lett. **57**, 1370 (1986).
[10] L. M. Falicov and J. C. Kimball, Phys. Rev. Lett. **22**, 997 (1969).

[11] R. Ramirez, L. M. Falicov, and J. C. Kimball, Phys. Rev. B **2**, 3383 (1970).
[12] M. Plischke, Phys. Rev. Lett. **28**, 361 (1972).
[13] J. K. Freericks, C. Gruber, and N. Macris, Phys. Rev. B **53**, 16189 (1996).
[14] J. W. Schweitzer, Phys. Rev. B **17**, 758 (1978).
[15] J. K. Freericks and R. Lemański, Phys. Rev. B **61**, 13438 (2000); L. Chen, J. K. Freericks, and B. A. Jones, *ibid.* **68**, 153102 (2003).
[16] N. Datta, R. Fernández, and J. Fröhlich, J. Stat. Phys. **96**, 545 (1999).
[17] P. Farkaŝovský, Phys. Rev. B **54**, 7865 (1996).
[18] C. A. Macedo, L. G. Azevedo, and A. M. C. de Souza, Phys. Rev. B **64**, 184441 (2001).
[19] J. K. Freericks and V. Zlatić, Rev. Mod. Phys. **75**, 1333 (2003).
[20] M. Suzuki and H. Takano, Phys. Lett. A **69**, 426 (1979).
[21] A. A. Migdal, Zh. Eksp. Teor. Fiz. **69**, 1457 (1975) [Sov. Phys. JETP **42**, 743 (1975)]; L. P. Kadanoff, Ann. Phys. (NY) **100**, 359 (1976).
[22] O. S. Sariyer, M. Hinczewski, and A. N. Berker, Phys. Rev. B **84**, 205120 (2011).
[23] J. Sznajd, Phys. Rev. B **63**, 184404 (2001).
[24] M. Suzuki, Phys. Lett. A **146**, 319 (1990).
[25] J. Sznajd, Phys. Rev. B **66**, 104420 (2002).
[26] C. E. T. Goncalves da Silva and L. M. Falicov, J. Phys. C: Solid State Phys. **5**, 906 (1972).
[27] D. K. Ghosh, Solid State Commun. **18**, 1377 (1976).
[28] W. Chung and J. K. Freericks, Phys. Rev. B **57**, 11955 (1998).
[29] M. M. Maśka and K. Czajka, Phys. Rev. B **74**, 035109 (2006).